Supporting Information

Margvelashvili et al. 10.1073/pnas.1316052110

Fig. S1. Dmanisi mandibles. High-resolution version of Fig. 2.

Fig. S2. D2600 pathologies. (*A*) RM1 periapical cyst. (*B*) RI2 periapical cyst. (*C*) Left canine hypercementosis. (Scale bars, 1 cm.)

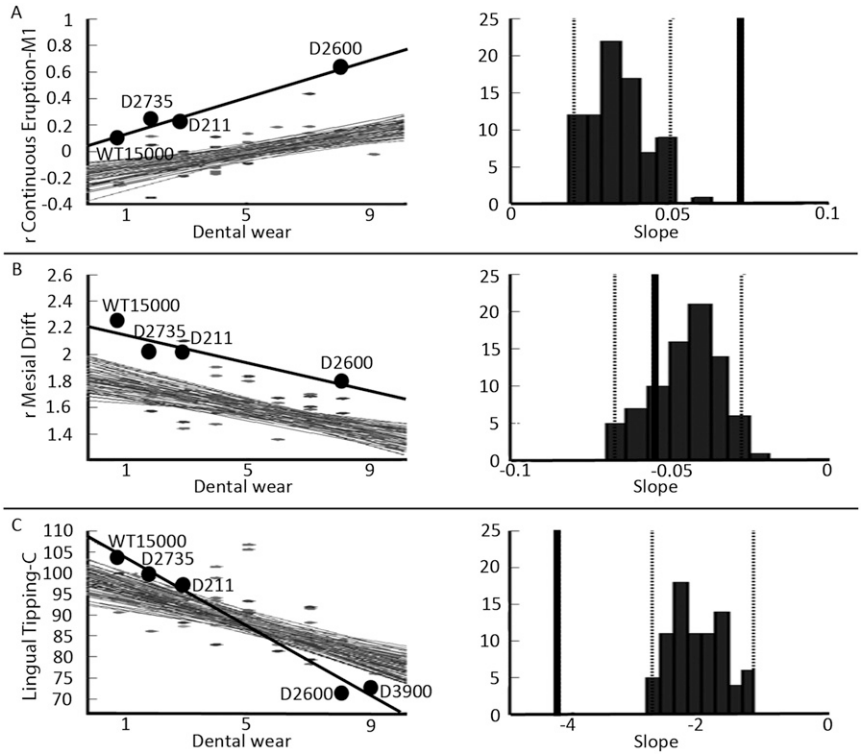

Fig. S3. Rates of wear-related dentoalveolar remodeling in early Pleistocene *Homo* versus modern *Homo sapiens*. (*A*) Relative continuous eruption of first molars. (*B*) Relative mesial drift. (*C*) Lingual tipping of canines. (*A*–*C*) (*Left*) Data for early Pleistocene *Homo* (Dmanisi and KNM-WT15000: filled circles, bold regression line) and modern humans (dashes, 80 resampled regression lines). (*Right*) Frequency distribution of resampled regression slopes in modern humans (black histogram). Dashed lines indicate 95% confidence interval; bold line indicates slope for early Pleistocene *Homo*. Resampling statistics are summarized in Table S5.

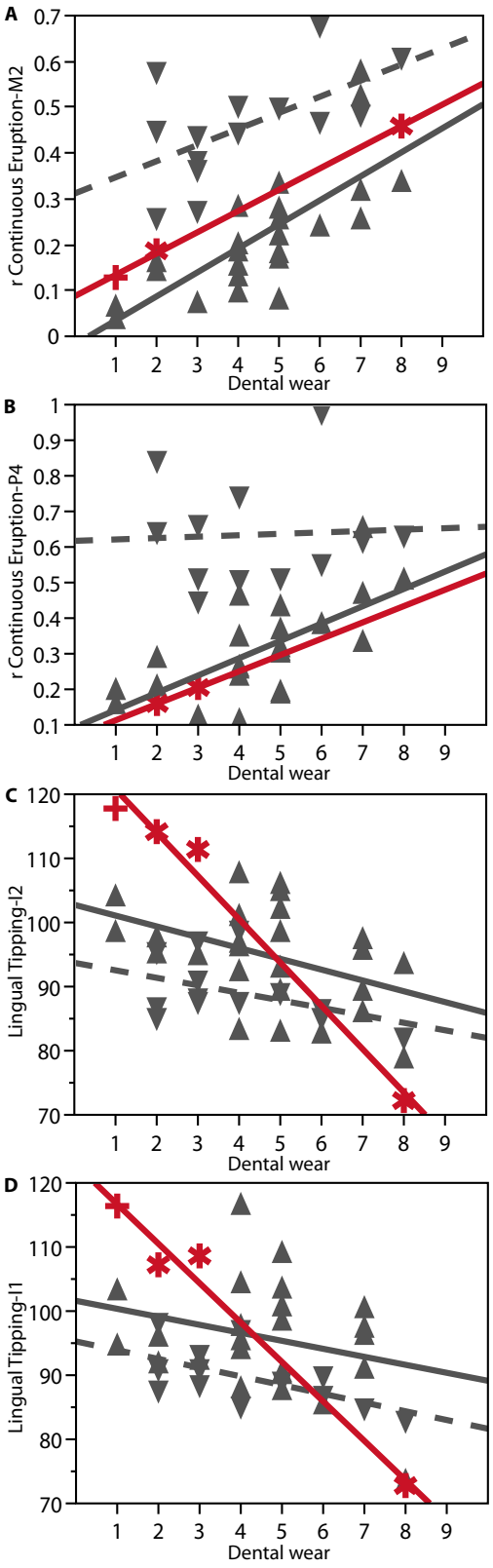

Fig. S4. Wear-related dentoalveolar remodeling in fossil *Homo* and modern humans: data for M2, P4, and incisors (I). (*A*) Relative continuous eruption of M2. (*B*) Relative continuous eruption of P4. (*C*) Lingual tipping of I2. (*D*) Lingual tipping of I1. Red symbols and regression lines, Dmanisi [stars, from left to right: D2735 (DW2), D211 (DW3), D2600 (DW8), D3900 (DW9)] and KNM-WT15000 (plus sign); gray symbols and lines, *H. sapiens* Australia (normal triangles and solid line) and Greenland (inverted triangles and dashed line). Regression statistics are summarized in Table S4.

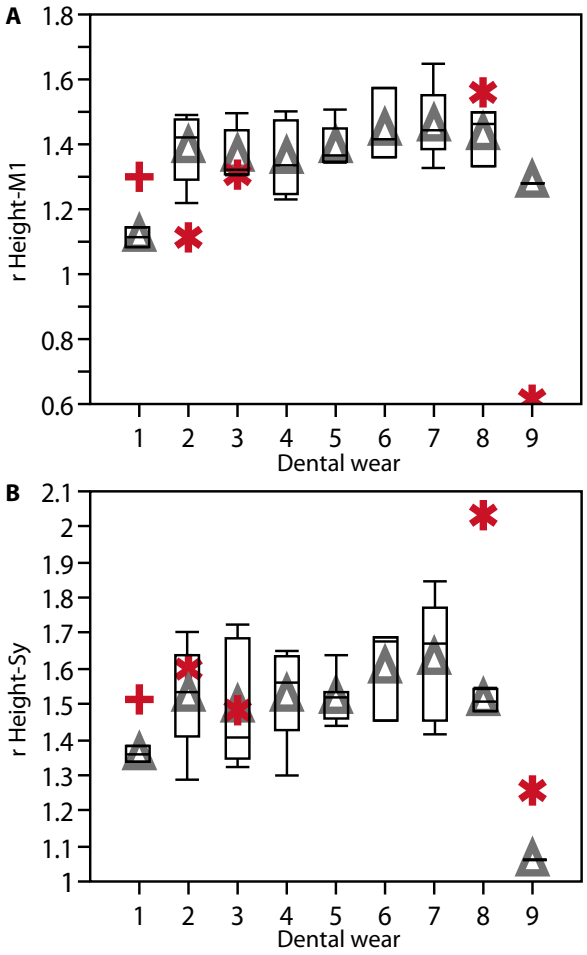

Fig. S5. Wear-related dentoalveolar remodeling in fossil *Homo* and modern humans: data for the mandibular corpus and symphysis. (*A*) Relative mandibular corpus height at M1. (*B*) Relative symphyseal height. Gray triangles, *H. sapiens* (Australians and Greenlanders) mean values (mean, SD, and range); red symbols, Dmanisi [stars, from left to right: D2735 (DW2), D211 (DW3), D2600 (DW8), D3900 (DW9)] and KNM-WT15000 (plus sign).

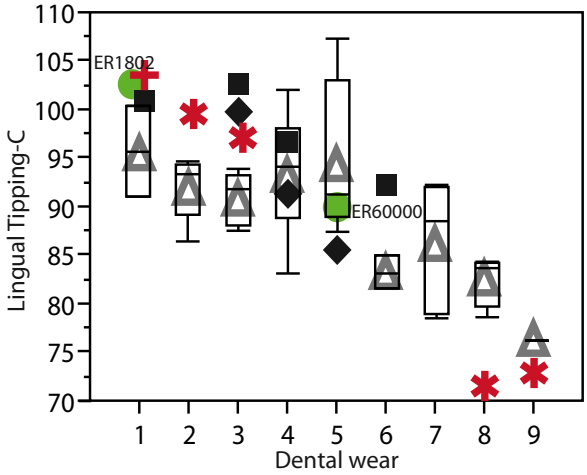

Fig. S6. Lingual tipping fossil *Homo* and modern humans: Gray triangles, *H. sapiens* mean values (mean, SD, and range); red symbols, Dmanisi [stars, from left to right: D2735 (DW2), D211 (DW3), D2600 (DW8), D3900 (DW9)] and KNM-WT15000 (plus sign); green circles, early Pleistocene *Homo* (KNM-ER 1802 and KNM-ER 60000) from Koobi Fora (1); black diamonds, Tighenif; black squares, Atapuerca Sima de los Huesos (SH).

1. Leakey MG, et al. (2012) New fossils from Koobi Fora in northern Kenya confirm taxonomic diversity in early *Homo*. *Nature* 488(7410):201–204.

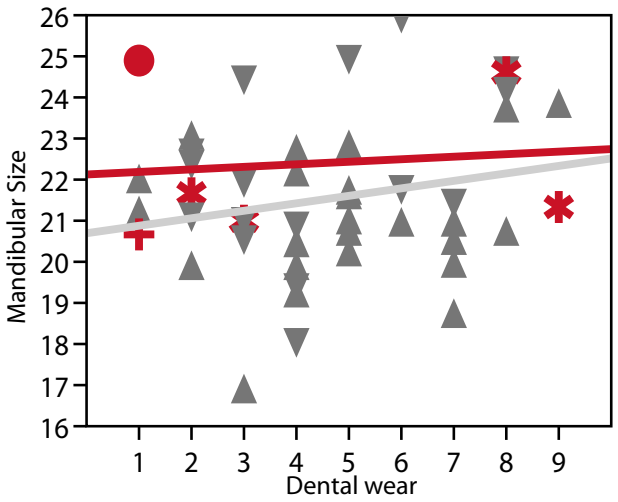

Fig. S7. Plot of mandibular size versus dental wear (DW) grade in fossil *Homo* and modern humans. Red symbols and regression line, Dmanisi [stars, from left to right: D2735 (DW2), D211 (DW3), D2600 (DW8), D3900 (DW9)], KNM-WT15000 (plus sign), and ER1808 (circle); gray symbols and light-gray line, *H. sapiens* Australia (normal triangles) and Greenland (inverted triangles). Regressions are nonsignificant. Early Pleistocene *Homo*, $r^2 = 0.013$ and $P = 0.8250$; *H. sapiens*, $r^2 = 0.04$ and $P = 0.1998$.

Table S1. Sample structure

Name	*n*	DW score	Species/group	Data*	Source
D2735		2	Early Pleistocene *Homo*	CT	GNM
D211		3	Early Pleistocene *Homo*	CT	GNM
D2600		8	Early Pleistocene *Homo*	CT	GNM
D3900		9	Early Pleistocene *Homo*	CT	GNM
KNM-WT15000		1	Early Pleistocene *Homo*	CT	KNM
KNM-ER1802		1	Early Pleistocene *Homo*	CT cast	KNM
KNM-ER60000		5	Early Pleistocene *Homo*	Lateral view	(1)
Tighenif	3	3–5	Mid-Pleistocene *Homo,* Africa	Lateral view	(2)
Atapuerca SH ($n = 4$)	4	1–6	Mid-Pleistocene *Homo,* Europe	Lateral view	(3, 4)
H. sapiens Australia	26	1–9	Recent *H. sapiens*	CT	LCHES
H. sapiens Greenland	15	1–8	Recent *H. sapiens*	CT	AIM

AIM, Anthropological Institute and Museum; CT, computed tomography (CT) measurements taken from CT data of original specimens (these specimens were used in all analyses); CT cast, measurements taken on CT scans of a cast; GNM, Georgian National Museum; KNM, National Museum of Kenya; Lateral view, measurements of LT-C taken from published lateral views; LCHES, Leverhulme Centre for Human Evolutionary Studies.

1. Leakey MG, et al. (2012) New fossils from Koobi Fora in northern Kenya confirm taxonomic diversity in early *Homo*. *Nature* 488(7410):201–204.
2. Schwartz JH, Tattersall I (2002) *The Human Fossil Record*: *Craniodental Morphology of Henus Homo (Africa and Asia)* (Wiley-Liss, Hoboken, NJ), Vol 2, pp 296–301.
3. Rosas A (1995) Seventeen new mandibular specimens from the Atapuerca/Ibeas Middle Pleistocene Hominids sample (1985–1992). *J Hum Evol* 28:533–559.
4. Rosas A (2001) Occurrence of neanderthal features in mandibles from the Atapuerca-SH site. *Am J Phys Anthropol* 114(1):74–91.

Table S2. List of the linear measurements analyzed

Measurement name	Measurement definition
Lingual tipping*	
C	Angle between the mandibular canal and main axis of the tooth/tooth socket
I2	Angle between the mandibular canal and main axis of the tooth/tooth socket
I1	Angle between the mandibular canal and main axis of the tooth/tooth socket
Continuous eruption	
M2	Distance between the lower-most point of the mandibular canal and lower-most point of the mesial portion of the mesial root-tip
M1	Distance between the lower-most point of the mandibular canal and lower-most point of the mesial portion of the mesial root-tip
P4	Distance between the lower-most point of the mandibular canal and lowermost point of the mesial portion of the root-tip
Mesial drift	
M2 distal to P3 mesial	Linear distance between the distal-most point of the M2 and mesial-most point of the P3 at the cervical level
Size	
Bilateral mental foramen	Bilateral length of the mental foramen measured at the central and lowermost point of the foramen
Symphyseal Thickness	Maximum thickness at pogonion
Foramen mentale height	Mean of left and right maximum length from the central and lowermost point of the foramen mentale
Size calculation	Geometric mean of bilateral width of mandible at mental foramen, symphyseal thickness, and foramen mentale height from the base of the mandible
Mandibular corpus height	
Height at M1	W150: minimum distance between the most inferior point on the base and the lingual alveolar margin at the midpoint of M1
Height at P4	W147: minimum distance between the most inferior point on the base and the lingual alveolar margin at the midpoint of P4
Height at symphysis	W141 and M69: minimum distance between the base of the symphysis and infradentale

All the measurements are taken form right (R) and left (L) sides of the mandible; all the figures and tables are based on R/L mean values, except when either side was unavailable or missing.

*Lingual tipping angle is measured, in lateral projection, between the nearly straight segment of the mandibular canal (in the central portion of the mandibular corpus) and the main axis of the tooth (root tip to crown tip), or the principal axis of the tooth socket (alveolar tip to midpoint of the ellipsoid formed by the alveolar border). See Table S3 for abbreviations.

Table S3. List of abbreviations

Abbreviation	Definition
C	Canine
Ce	Cementum
CE	Continuous eruption
CT	Computed tomography
DW	Dental wear
En	Enamel
I	Incisor
JEOL	Japan Electron Optics Laboratory
L	Left
LEH	Linear enamel hypoplasia
LT	Lingual tipping
M	Molar
MD	Mesial drift
MS	Mandibular size
P	Premolar
R	Right
rCE	Relative continuous eruption
rH	Relative corpus height
rMD	Relative mesial drift
SEM	Scanning electron microscope
TMJ	Temporomandibular joint

Table S4. Regression and resampling statistics for Fig. 4 and Fig. S4

Species/group	Statistics	rCE-M1	rMD	LT-C	rH-M1	rCE-M2	rCE-P4	LT-I2	LT-I1	rH-P4
Australians	r^2	0.43	0.23	0.3	0.23	0.52	0.41	0.18	0.07	0.3
	P	0.0004	0.0159	0.0039	0.0177	0.0001	0.0009	0.033	0.195	0.0071
Greenlanders	r^2	0.33	0.15	0.46	0.25	0.45	0.05	0.19	0.36	0.16
	P	0.0211	0.1363	0.0058	0.0461	0.0087	0.4821	0.136	0.029	0.1241
Early Pleistocene *Homo*	r^2	0.98	0.84	0.98	0.7	0.99	—	0.98	0.97	0.62
	P	0.0121	0.0817	0.0011	0.16	0.0119	—	0.01	0.013	0.21
Tighenif	r^2			0.98						
	P			0.0693						
Atapuerca SH	r^2			0.7						
	P			0.1575						

See Table S3 for abbreviations.

Table S5. Regression and resampling statistics for Fig. S3

Species/group	Statistics	rCE-M1	rMD	LT-C
H. sapiens	Slope	+0.023	−0.066	−2.27
		+0.05	−0.026	−1.279
Early Pleistocene *Homo*	Slope	+0.07	−0.054	−4.19

See Table S3 for abbreviations.